Polymer Chemistry

Accepted Manuscript

ROYAL SOCIETY OF CHEMISTRY

www.rsc.org/polymers

Cite this: DOI: 10.1039/c0xx00000x

www.rsc.org/xxxxxx

ARTICLE TYPE

π-conjugated sulfonium-based photoacid generators: an integrated molecular approach for efficient one and two-photon polymerization

Ming Jin,*[a] Hong Hong,[a] Jianchao Xie,[a] Jean-Pierre Malval,*[b] Arnaud Spangenberg,[b] Olivier Soppera,[b] Decheng Wan,[a] Hongting Pu,[a] Davy-Louis Versace,[c] Tiffanie Leclerc,[b] Patrice Baldeck,[d] Olivier Poizat[e] and Stephan Knopf [b]

Received (in XXX, XXX) Xth XXXXXXXXX 20XX, Accepted Xth XXXXXXXXX 20XX
DOI: 10.1039/b000000x

The cationic photoinitiating abilities of a series of 'push-pull' sulfonium-based photoacid generators (PAG) have been investigated. In this linear π-conjugated series, a 4-N,N-diphenylaminostilbene subunit is associated to different types of sulfonium substituents which are connected to the stilbene moiety either in 4' position or in 3' position. This para-to-meta substitution effect leads to a strong increase of the quantum yield for acid generation with a maximum value of ca. 0.5. Such a positioning effect has a strong influence on the efficiency of the S-C bond cleavage. A detailed photolysis mechanism has been proposed. By contrast to commercially available sulfonium salts, these highly reactive π-conjugated PAG all exhibit a large absorption in visible range as well as large two-photon absorption cross-sections (δ_{MAX} > 600 GM) in the near-infrared region. As a consequence, efficient one and two-photon polymerizations are observed at 405 nm and 800 nm respectively using typical monomers such as cyclohexene oxide, n-butyl vinyl ether or SU-8 photoresist. By fabrication of well resolved two-dimensional microstructures, we finally demonstrate the potential use of these new generations of PAG in the fields of one and two-photon lithography.

Introduction

The photoinitiated cationic polymerization[1-3] is currently used in a very large field of applications such as coating, photoresists, printing plates, integrated circuits, laser-induced 3D curing, nanoscale micromechanics and adhesive. In this context, photoacid generators (PAG) constitute an important class of cationic photoinitiators which have a strategic position in the polymer industry[4,5]. Upon direct irradiation, photoacid generators undergo photolysis to form a protic acid. The primary bond photodissociation within the molecular structure of this photoinitiator generally implies a relatively high energy in such manner that most of commercial PAG are photoactivated at wavelengths ranging from VUV to close UV[6-8]. It is clearly a major drawback which limits the use of PAG within a restricted part of the spectral range. Moreover, their low absorptivity in the visible region rules out the use of low-cost excitation sources, such as visible LED or excludes the possibility of conducting polymerizations at ambient sunlight[9-11]. Therefore, extending the absorption propensity of PAG to the visible range with the preservation of the photoreactivity clearly constitutes a fundamental issue. Parallel to this challenge, a concomitant use of these new PAG for near-infrared (NIR) phototopolymerization can be demonstrated using two-photon excitation mode. In this emergent technology[12-15], the NIR beam of an ultrafast laser is tightly focused into a prepolymer resin. Taking advantage of the very low probability for the two-photon absorption (2PA) event, a spatial confinement of all primary and subsequent photo-induced processes is promoted. The NIR photopolymerization is then localized within the focal volume of the laser which allows the fabrication of 2D or 3D microstructures of arbitrary complexities.

In the past decades, many efforts have been done to extend the use of PAG toward the visible and NIR ranges[1]. Two main strategies were developed. The first one, namely the sensitizing method[16,17], consists in associating a visible light sensitizer, such as thioxanthone[16,18], coumarin[19], or phenothiazine[20], with a commercial PAG, such as onium salts. The acid generation proceeds through a photoinduced electron transfer (PeT) from the excited chromophores to the PAG. Another elegant strategy, namely the free radical promoted cationic polymerization (FRPCP)[9,21-30], concerns the use of photogenerated radicals (R•) as strong reductants which are oxidized by iodonium or sulfonium salts. All these sensitizing methods can be directly transposed to two-photon excitation[31-38]. However, despite their facile and economic processing steps, it should be emphasized that these multicomponent systems generally lead to additional problems associated with solubility, monomer compatibility, and migration. In addition, the global kinetics of this method is intrinsically limited by diffusion; even the most promising FRPCP had to tackle with oxygen inhibition issues. Therefore, a second strategy based on molecular engineering has been alternatively proposed[39-45]. In order to improve the photoreactivity with the increase of linear and non-linear

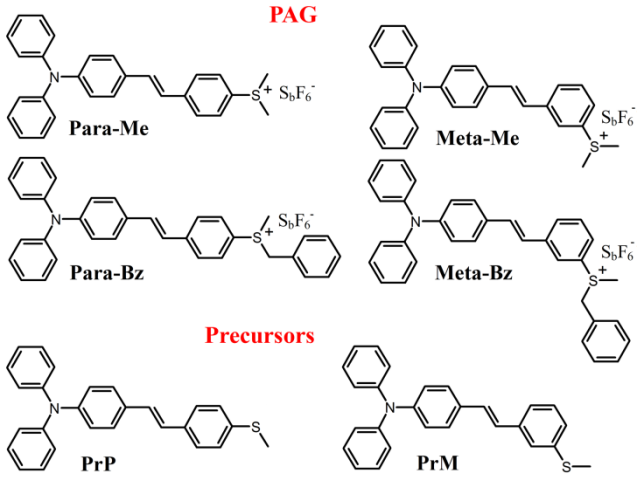

Scheme 1 Molecular structures of PAG and precursors.

absorption properties, various photocleavable subunits have been methodically implemented into a large panel of π-conjugated systems[39-44]. For example, Saeva *et al.*[46-49] reported several reactive sulfonium-based PAG incorporating anthracenyl and naphthacenyl subunits which are photoactivable in the 390-490 nm range. Perry *et al.*[39,43,44] also designed a sulfonium-based bis[(diarylamino)styryl] benzene derivative with a maximum absorption at 390 nm which both presents a high quantum yield for acid generation ($\Phi_H^+ \sim 0.5$) and a large 2PA cross-section (δ ~ 700 GM). In the same manner, Belfield *et al.*[42,45] developed a 1,8-bis(4'-styryl)fluorene with two para-substituted diphenylsulfonium groups at both extremities of the PAG. Even though this molecular architecture is similar to the previous one (i.e. A-π-A), the quantum yield for acid generation drops to a value 6 times lower due to a positioning effect of the sulfonium substituent. More recently our working group confirmed this positioning effect with the elaboration of several D-π-A sulfonium-based PAG (Scheme 1) in which a strong enhancement of Φ_H^+ was demonstrated through a para-to-meta positioning effect of the sulfonium substituent[50].

In the present contribution, we give a qualitative and tentative mechanistic explanation of these PAG and correlate their photoreactivities with their respective photoinitiating performances. This analytical investigation has been both performed upon one and two-photon absorption processes using various monomers. We will finally demonstrate the potential interest of this new series of PAG for one and two-photon lithography applications.

Experimental section

Materials and characterization

All chemicals for synthesis were purchased from Sinopharm Chemical Reagent Co., Ltd., TCI, Alfa Aesar, or J&K Chemical. They were used without further purification unless otherwise specified. The monomer cyclohexene oxide (CHO, 98%, Aldrich), n-butyl vinylether (BVE, >97%, Fluka) were distillated over CaH_2 in vacuum. The cycloaliphatic diepoxide monomer, namely 3,4-Epoxycyclohexylmethyl-3,4-epoxycyclohexane-carboxylate (EPOX, >98 %) was supplied by Aldrich. The SU-8 resin without PAG was provided by NanJing Baisiyou Tech. Co., Ltd. All the solvents employed for photophysical measurements were Aldrich, Fluka or Merck spectroscopic grade.

Proton and carbon magnetic resonance spectra (^{1}H, ^{13}C NMR) were recorded on a Bruker Avance 500 (400 MHz) spectrometer. Chemical shifts were reported in parts per million (ppm) downfield from the Me_4Si resonance which was used as the internal standard when recording NMR spectra. Mass spectra were recorded on a Micromass GCTTM. The molecular weights of photopolymers were determined using a GPC instrument equipped with MZ-Gel SD plus columns (HR series 3, 4, 5E) with THF as eluent at a flow rate of 1 mL/min and a water 410 Differential refractometer detector.

Synthesis of the PAG

The detailed synthetic routes for the stilbene-based sulfonium salts have been reported in our previous paper[50]. In order to study these PAG as cationic photoinitiators, the initial counterion $CF_3SO_3^-$ was replaced by $S_bF_6^-$ according to an ion-exchanging method described in reference[51]. Indeed, Zhou *et al.*[51] clearly demonstrated that the cationic photopolymerization of epoxide resins leads to a more efficient epoxy ring-opening reaction with $S_bF_6^-$ as counterion than with $CF_3SO_3^-$.

(*E*)-(4-(4-(diphenylamino)styryl)phenyl)dimethylsulfonium hexafluoroantimonate (Para-Me).

The yield: 86.0%. ^{1}H NMR (CD_3CN, δ_{ppm}): 7.86~7.80 (m, 4H, PhH); 7.51 (d, *J = 8.6 Hz*, 2H, PhH); 7.38 (d, *J = 16.4 Hz*, 1H, CH=CH); 7.32 (m, 4H, PhH); 7.14 (d, *J = 15.9 Hz*, 1H, CH=CH); 7.09 (m, 6H, PhH); 7.00 (d, *J = 8.7 Hz*, 2H, PhH); 3.12 (s, 6H, CH_3). ^{13}C NMR (CD_3CN, δ_{ppm}): 149.27; 148.09; 144.88; 133.57; 131.17; 130.92; 130.42; 128.99; 128.88; 125.71; 124.87; 124.59; 123.27; 122.94; 29.43. EI-MS (m/z): calcd for $C_{28}H_{26}F_6NSS_b$, 643.0728, found: 408.1754, [M - $S_bF_6^-$]$^+$; Anal. calcd for $C_{28}H_{26}F_6NSS_b$: C, 52.19; H, 4.07; N, 2.17; Found: C, 52.35; H, 4.15; N, 2.17.

(*E*)-(3-(4-(diphenylamino)styryl)phenyl)dimethylsulfonium hexafluoroantimonate (Meta-Me).

The yield: 84.0%. ^{1}H NMR (CD_3CN, δ_{ppm}): 8.03 (s, 1H, PhH); 7.89 (d, *J = 7.6 Hz*, 1H, PhH); 7.73 (d, *J = 7.7 Hz*, 1H, PhH); 7.67 (t, *J = 7.8 Hz, 7.9 Hz*, 1H, PhH); 7.63 (d, *J = 22.9 Hz*, 1H, CH=CH); 7.48 (d, *J = 8.6 Hz*, 2H, PhH); 7.36~7.29 (m, 5H; PhH and CH=CH); 7.14~7.07 (m, 6H, PhH); 7.01 (d, *J = 8.6 Hz*, 2H, PhH); 3.15 (s, 6H, CH_3). ^{13}C NMR (CD_3CN, δ_{ppm}): 149.14; 148.23; 141.79; 132.73; 132.49; 132.03; 131.20; 130.48; 128.88; 128.69; 127.70; 126.80; 125.71; 125.79; 124.80; 124.58; 124.53; 29.26. EI-MS (m/z): calcd for $C_{28}H_{26}F_6NSS_b$, 643.0728, found: 408.1783, [M - $S_bF_6^-$]$^+$; Anal. calcd for $C_{28}H_{26}F_6NSS_b$: C, 52.19; H, 4.07; N, 2.17; Found: C, 52.38; H, 4.05; N, 2.19.

(*E*)-benzyl(4-(4-(diphenylamino)styryl)phenyl)(methyl)sulfonium hexafluoroantimonate (Para-Bz).

The yield: 83.0%. ^{1}H NMR (CD_3CN, δ_{ppm}): 7.75 (d, *J = 8.6 Hz*, 2 H, PhH); 7.64 (d, *J = 8.6 Hz*, 2H, PhH); 7.49 (d, *J = 8.6 Hz*, 2H, PhH); 7.43 (d, *J = 7.3 Hz*, 1H, PhH); 7.38 (d, *J = 7.6 Hz*, 2H, ZHPhH); 7.33 (m, 5H, PhH); 7.22 (d, *J = 7.2 Hz*, 2H, PhH); 7.09 (m, 7H, PhH); 7.00 (d, *J = 8.6 Hz*, 2H, PhH); 4.83 (d, *J = 12.8 Hz*, 1H, CH_2); 4.67 (d, *J = 12.8 Hz*, 1 H, CH_2); 3.14 (s, 3H, CH_3). ^{13}C NMR (CD_3CN, δ_{ppm}): 148.27; 133.48; 132.29; 131.64; 131.12; 130.56; 130.39; 130.34; 129.16; 128.93; 125.92; 124.94; 124.88; 124.78; 123.37; 29.62; 25.87. EI-MS (m/z): calcd for $C_{34}H_{30}F_6NSS_b$, 719.1041, found: 484.2090 [M - $S_bF_6^-$]$^+$; Anal.

calcd for $C_{34}H_{30}F_6NSSb$: C, 56.68; H, 4.20; N, 1.94; Found: C, 56.35; H, 4.38; N, 1.87.

(*E*)-benzyl(3-(4-(diphenylamino)styryl)phenyl)(methyl)sulfonium hexafluoroantimonate (Meta-Bz). The yield: 77.4%. ^{1}H NMR (CD_3CN, δ_{ppm}): 7.86 (d, *J = 7.6 Hz*, 1H, PhH); 7.80 (s, 1H, PhH); 7.59 (t, *J =7.6 Hz*, *8.8 Hz*, 1H, PhH); 7.51 (d, *J = 8.8 Hz*, 1H, PhH); 7.47 (d, *J = 8.8 Hz*, 2H, PhH); 7.31-7.44 (m, 8H, PhH); 7.23 (m, 3H, PhH); 7.10 (m, 6H, PhH); 7.00 (d, *J = 8.6 Hz*, 2H, PhH); 4.88 (d, *J = 12.8 Hz*, 1H, CH_2); 4.72 (d, J = 12.8 Hz, 1H, CH_2); 3.18 (s, 3H, CH_3). ^{13}C NMR (CD_3CN, δ_{ppm}): 149.11; 148.19; 141.68; 132.98; 132.49; 131.85; 131.62; 131.14; 131.04; 130.47; 130.23; 129.71; 128.87; 128.61; 128.30; 125.69; 124.66; 124.57; 123.96; 123.49; 51.67; 25.41. EI-MS (m/z): calcd for $C_{34}H_{30}F_6NSSb$, 719.1041, found: 484.2093 [M - SbF_6^-]$^+$; Anal. calcd for $C_{34}H_{30}F_6NSSb$: C, 56.68; H, 4.20; N, 1.94; Found: C, 56.30; H, 4.36; N, 1.85.

Instrumentation and methods

The UV-Visible spectra were recorded on a Mapada UV-6300 spectrophotometer. The steady-state fluorescence experiments were performed on a Varian Cary Eclipses fluorescence spectrometer. Emission spectra are spectrally corrected, and fluorescence quantum yields include the correction due to solvent refractive index and were determined relative to quinine bisulfate in 0.05 molar sulfuric acid (Φ_{fluo} = 0.52)[52]. Photolytic reactions were performed by irradiation of N_2-degassed solutions containing the PAG with a 405 nm LED Spot Curing System (UVATA, Shanghai).

The cationic photopolymerizations were performed using two distinctive methods: *a)* Aliquots (1.0 mL) of a methylene chloride solution containing 3.2 × 10^{-3} M of PAG and 7.9 M of cyclohexene oxide or butyl vinyl ether were sealed in 4-mL capped vials and irradiated at 405 nm in a merry-go-round holder. After a defined time of irradiation, all reactions are stopped by immediate addition of 1 mL of 2 M ammonia in methanol. The polymer was then precipitated in methanol, collected by filtration and dried in vacuum for 40 h. The conversion of monomer was determined gravimetrically. *b)* The kinetics of photopolymerization was monitored *in situ* by Fourier transform real-time infrared spectroscopy (FT-RTIR) with a Thermo-Nicolet 6700 instrument IR-spectrometer. A drop of the photocurable formulation was deposited on a KBr pellet then spread out with a calibrated bar. The aerated film was irradiated at 405 nm with the LED source or using a Xe-Hg lamp (Hamamatsu, L8252, 150 W) equipped with a band pass filter. The conversion rates are derived from the changes in the infrared absorption bands of the monomer. The regions of interest correspond to the decrease in the epoxide absorption bands in the 800-900 cm^{-1} region which correspond to the C-H bond stretching vibration of epoxide and to the increase of the peaks at 1050-1150 cm^{-1} assigned to the absorption of the (C-O-C) groups in the poly(ether) which is produced upon photopolymerization[53].

The one-photon lithography was performed using SU-8 photoresist (SU-8 2005 from NanJing Baisiyou Tech. Co., Ltd) which was specifically purchased without any photoinitiator. The photoresist was mixed with Meta-Bz (1 wt %). The formulation was spin-coated on glass substrates leading to regular films

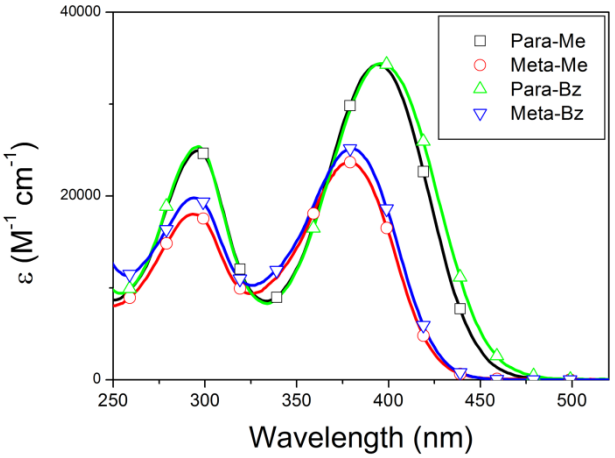

Fig. 1 Absorption spectra of PAG in acetonitrile.

whose thickness (~ 1 μm) was measured by profilometry. The irradiation exposure dose at 405 nm was fixed at 200 μJ cm^{-2}. The procedure for photolithography can be described as follows: *(i)* Spin-coating (3000 rpm) on a Si substrate which was previously pre-treated upon immersion into a piranha solution during 3h at 80 ℃. *(ii)* Edge bead removal and 3 min soft baking at 90 °C. *(iii)* Photopatterning upon visible irradiation at 405 nm during 8 s. *(iv)* 3 min post-baking at 90 ℃ leading to the appearance of the μ-structures *(v)* Final development by rinsing with isopropanol or with cyclohexanone.

The same procedure was used to prepare the films for two-photon lithography. The two-photon microfabrication was carried out using a Zeiss Axio Observer D1 inverted microscope. The two-photon excitation was performed at 800 nm using a mode-locked Ti: Sapphire oscillator (Coherent, Chameleon Ultra II: pulse duration: ~140 fs; repetition rate: 80 MHz). The incident beam was focused through a 0.65 NA objective (40 ×) which leads to radial spot sizes of 600 nm at λ_{exc} = 800 nm ($1/e^2$ Gaussian). The film was mounted on a 3D piezoelectric stage allowing the translation relative to the laser focal point. The intensity of the entering laser was controlled with the use of an acousto-optic modulator. The displacement of the sample and all photonic parameters (i.e. excitation power and irradiation time) were computer-controlled. This entire lithography set-up was purchased from Teemphotonics Company.

Results and discussion

Photophysical properties and mechanism for acid photogeneration

Fig. 1 shows the absorption spectra of all PAG in acetonitrile. The corresponding spectroscopic data are listed in Table 1. As expected, all chromophores exhibit an intensive band located in the 350−450 nm range. Interestingly, the meta-to-para substituent effects both induce a remarkable increase of the band intensity associated with a clear bandshift to the low energy region (~ 1000 cm^{-1}) in Methyl-containing and Benzyl-containing PAG (Scheme 1). These spectral effects were ascribed to a better electronic delocalization between the donor (i.e. N, N-diphenylamine) and acceptor (i.e. phenylsulfonium) groups in Para-substituted PAG. It should be noted that methyl to benzyl substitution on the sulfonium groups hardly influences the absorption spectra which

Table 1 Summary of optical data and parameters of PAG and Precursors in acetonitrile.

	λ_{abs} / nm	ε_{max} / M^{-1} cm^{-1}	Φ_{fluo}	Φ_H^+	δ_{max} (λ_{max}) [a] / GM (nm)
Para-Me	395	34300	0.16	0.007	643 (870)
Meta-Me	381	23700	-	0.43	650 (800)
Para-Bz	397	34400	-	0.25	650 (880)
Meta-Bz	379	25200	-	0.50	648 (800)
PrP	370	37700	0.73	-	-
PrM	366	22900	0.64	-	-

[a] from Reference[50].

both suggests that the presence of a crowded substituent (i.e. benzyl) does not induce strong structural changes at ground state and that the electron withdrawing ability of a dimethylsulfonium group is equivalent to that of a benzylmethylsulfonium one. In addition to the presence of this intensive band, such N-phenylated chromophores also exhibit a second distinctive band near 300 nm which is a consequence of electronic transitions mainly centered on the triphenylamine moieties[54]. In parallel to their strong linear absorption within the visible range (ε_{max} ~ 24000 to 34000 M^{-1} cm^{-1}), these D-π-A chromophores also exhibit relatively high two-photon absorption cross-sections (δ) in the NIR region (δ_{max} ~ 650 GM)[50]. Interestingly, all PAG exhibit equivalent δ_{max} (Table 1) which suggests that the para-to-meta positioning effect does not have detrimental influence on the 2PA properties as previously demonstrated on comparable series[41].

The quantum yields for photoacid generation (Φ_H^+) which are reported in Table 1 have been measured in acetonitrile using rhodamine B as acid indicator according to the method reported by Scaiano *et al.*[55] One clearly observes that the efficiency for acid generation is strongly dependent on the position of the sulfonium group. For instance, Φ_H^+ undergoes a 60-fold increase on going from Para-Me to Meta-Me. This para-to-meta substitution effect has been previously attributed to a strong increase of the energy gap between the S_1 (σ*) and S_2 (π*) excited states[46-48]. Indeed, a better energy separation of the two excited states should limit their vibronic interactions which preserve the dissociating character of the lowest excited state. Interestingly, the quantum yield of Para-Bz (Φ_H^+ = 0.25) is much higher than that of Para-Me. This effect can be attributed to a better leaving propensity of the benzyl group as compared to that of the methyl[56]. Fig. 2A shows the typical evolution of the absorption spectra of Para-Bz in acetonitrile upon irradiation at 405 nm. Whereas the band located around 300 nm remains invariant, the longest wavelength absorption band dramatically collapses with the appearance of a less intensive band located at 370 nm. Moreover upon the photolysis, a highly fluorescent by-product is progressively generated (Fig. S1, ESI†). The excitation spectrum recorded at the maximum fluorescence wavelength matches perfectly the absorption spectrum of the precursor PrP which presents a distinctive band at 370 nm (Fig. S2, ESI†). The presence of this precursor was also confirmed by ^{1}H NMR upon irradiation of Para-Bz in d_3-acetonitrile. Interestingly, the ^{1}H NMR and HPLC analyses also indicate that the yield for generation of PrP is strongly increased when the photolysis is performed in presence of 10 equivalent of triethylamine (TEA) (Fig. S3-5, ESI†). As shown in Fig. 2B, this effect is corroborated by the strong increase of the absorption band of PrP (λ_{max} at 370 nm) upon the photolysis of Para-Bz in presence of TEA (10 eq.).

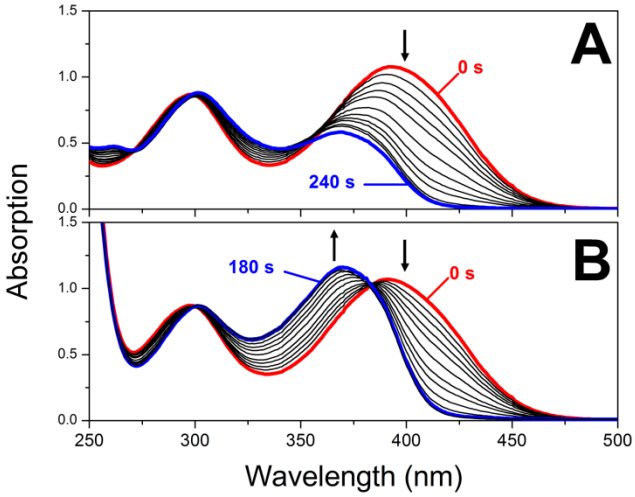

Fig. 2 Evolution of the absorption spectra of Para-Bz (3.1×10^{-5} M) upon irradiation at 405 nm (0.25 mW cm^{-2}). **A**: without Et_3N. **B**: in presence of 10 eq. of Et_3N. (Solvent: acetonitrile).

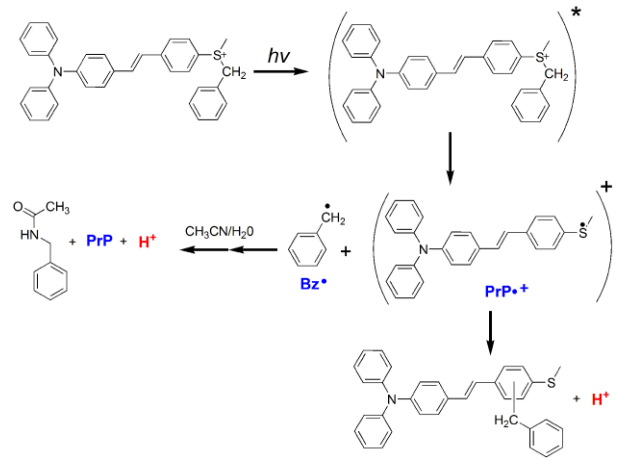

Scheme 2. Proposed photolysis mechanism for Para-Bz.

Note that the same effects are observed for all PAG as displayed in Fig. S6. Similarly to the mechanism established by Saeva *et al.*[46-48] for phenylanthracene or phenlynaphtacene sulfonium salts, we proposed that the photogeneration of acids mainly stems from an intramolecular rearrangement initially promoted by a photoinduced electron transfer (PeT) from the amino group to sulfonium one. As previously demonstrated[50], this PeT process is largely exothermic and should lead to a reductive carbon-sulfur σ-bond cleavage. For benzyl substituted PAG, for instance, the PeT process should lead to the production of a benzyl radical (Bz•) and the radical cation of the precursor ($PrP^{\bullet+}$) as illustrated in Scheme 2. The benzyl radical known as a good leaving group[56] can presumably migrate from sulfur to all aromatic carbon bearing an hydrogen atom. A final recombination reaction between Bz• and $PrP^{\bullet+}$ should promote the release of a proton. It should be emphasized that the further stability of the generated radical cation should certainly counterbalance the efficiency of the cross-coupling reaction. According to their respective resonance forms, it is clear that the para-substituted radical cation exhibits a higher stability than its meta homologue. Such a difference in stability is also in line with the higher Φ_H^+ observed for meta derivatives.

Table 2 Effective acid generation efficiencies upon one and two-photon induced excitation at 405 nm and 800 nm, respectively. Maximum 1PA polymerization rates (R_p/M_0) and two-photon polymerization thresholds (E_{th}) in **EPOX** resins.

PAG	1PA		2PA	
	$\Phi_{H^+}.\varepsilon_{405nm}$ [a] / M^{-1} cm^{-1}	$R_p/[M_0]$ [b] / s^{-1}	$\Phi_{H^+}.\delta_{800nm}$ [a] / GM	E_{th} [b] / µJ
Para-Me	220	0.3	2	25
Meta-Me	8800	2.7	270	10
Para-Bz	7900	1.5	93	22
Meta-Bz	11600	3.6	310	10

[a] in acetonitrile. [b] in **EPOX** resin.

The mass spectrum (MS) analysis of the final products obtained from the total photolysis of Para-Bz in acetonitrile in the presence of TEA has been performed and the corresponding spectrum is displayed in Fig. S5. One clearly observes a peak at *m/z* = 484.2 which can be confidently attributed to the cross-coupling product. As previously indicated, the presence of TEA strongly competes with the final rearrangement since a strong increase for the generation of PrP was observed. This is also in line with the MS analysis which confirms that the major product is PrP (*m/z* = 394.2). Interestingly two other by-products are clearly detected at *m/z* = 150.1 and *m/z* = 192.2. The low mass product corresponds to the N-(benzyl)acetamide. A similar derivative (i.e. N-(4-cyanobenzyl)acetamide) has been previously identified by Saeva et al.[46,47,57,58] in equivalent conditions. It can be ascribed, in our case, to a thermodynamically allowed back electron transfer process between PrP•+ (E_{ox} = 0.95 V, SCE) and Bz• (E_{ox} = 0.73, SCE[59]) which leads to PrP and a benzyl cation. This latter cation can then react with acetonitrile and residual water to finally generate the acetamide derivative and a proton[57,58] (see Scheme 2). The second low mass product is very interesting since it indirectly clarifies the perturbative role of TEA in the global mechanism. Indeed, this second product should simply correspond to a recombination reaction between Bz• and TEA cation as follows:

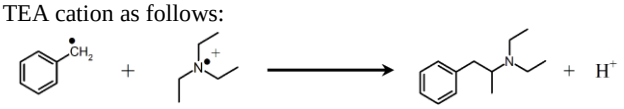

Interestingly, the presence of TEA•+ suggests that the amine should be first oxidized presumably by PrP•+ which therefore corroborates the strong increase in the generation of PrP in presence of a large excess of TEA (10 eq.).

Hence several conclusions can be drawn from this global mechanism. The acid generation proceeds through a photoinduced intramolecular electron-transfer bond cleavage which produces a radical cation/radical pair. The subsequent rearrangement of these two transient species promotes the H^+ release. The efficiency for acid generation is both dictated by the para/meta position of the sulfonium group and also by the nature of the substituent on the sulfur atom (i.e. benzyl vs. methyl). Such structural changes should have strong consequences on the photoinitiating reactivity as will be highlighted hereafter.

One and two-photon initiating polymerizations

It should be first indicated that a relevant criterion to evaluate the relative performances of the photoacid generators consists in determining the effective efficiency for H^+ photogeneration. This fundamental criterion corresponds to the product of Φ_{H^+} by ε_λ (1PA) or $\delta_{\lambda'}$ (2PA). The latter parameters represent the one or two photon induced ability to generate excited species upon excitation at λ (1PA) or λ' (2PA) respectively whereas the first factor indicates the efficiency for producing H^+ from the excited species. In Table 2, the corresponding values are reported for $\Phi_{H^+}.\varepsilon_{405\ nm}$ and $\Phi_{H^+}.\delta_{800\ nm}$. First, it clearly appears that all meta PAG have superior efficiencies than their para homologues. Moreover, even though the benzyl substituent is a better leaving group than the methyl one, we observe that Meta-Me leads to a higher effective acid photogeneration than Para-Bz. In order to corroborate these preliminary trends with the effective photoinitiating efficiencies of the PAG, cationic photopolymerizations have been first performed in a difunctional epoxide monomer (EPOX, see Scheme 3) upon one-photon excitation at 405 nm and two-photon excitation at 800 nm. Fig. 3 shows the FT-RTIR kinetic curves during visible irradiation of the formulations containing the PAG (1 wt %). The corresponding values for the maximum polymerization rate ($R_p/[M_0]$) are reported in Table 2. The photoinitiation efficiencies can be clearly correlated with $\Phi_{H^+}.\varepsilon_{405nm}$. For instance, the meta PAG both leads to a rapid photopolymerization up to 45 % conversion of epoxide functions after 90 s of irradiation. Para-Bz exhibits a comparable kinetic curve but with a lower $R_p/[M_0]$ and a final conversion of about 40 % after 180 s of irradiation. Finally, Para-Me whose $\Phi_{H^+}.\varepsilon_{405nm}$ is more than one order of magnitude lower than those of the other PAG shows a slow dynamic of conversion with an initial induction period (~ 20 s) and a final conversion of 30 %.

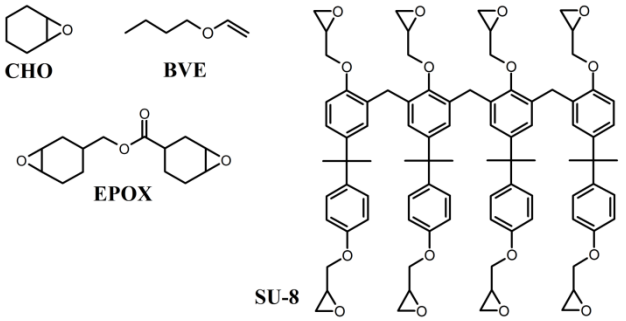

Scheme 3. Molecular structures of monomers.

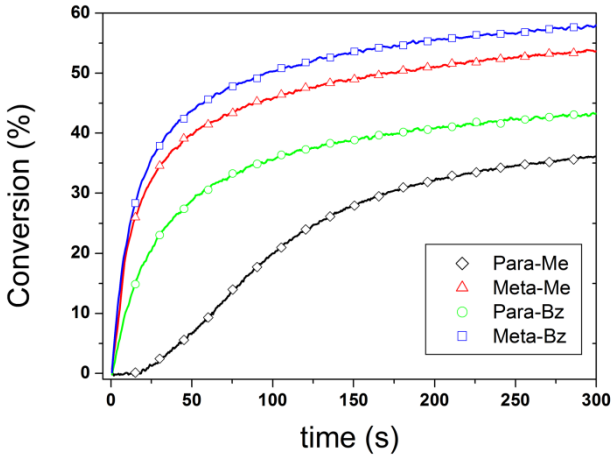

Fig. 3 Conversion vs. time curves for cationic photopolymerization of diepoxide monomer EPOX containing PAG (1 wt %). λ_{exc}: 405 nm , Irradiance: 5 mW cm^{-2}.

Table 3 Molecular weights of polymers obtained upon various photopolymerization conditions.

PAG	Monomer **M**	**[M]** % wt	**[PAG]** % wt	Intensity mW cm^{-2}	Conversion [d] %	M_n [f]	M_w/M_n
Para-Bz	**CHO**	37 [a]	0.6	0.2	44.3	2830	1.63
Meta-Bz	**CHO**	37 [a]	0.6	0.2	46.2	4170	1.55
Para-Bz	**BVE**	37 [a]	0.6	0.2	80.4	19500	2.07
Meta-Bz	**BVE**	37 [a]	0.6	0.2	87.3	43200	1.60
Para-Bz	**CHO**	37 [a]	0.6	2.0	58.8	14100	2.53
Meta-Bz	**CHO**	37 [a]	0.6	2.0	35.9	3360	2.12
Para-Bz	**BVE**	37 [a]	0.6	2.0	78.2	10200	2.67
Meta-Bz	**BVE**	37 [a]	0.6	2.0	75.1	5140	2.13
Meta-Bz	**CHO**	Bulk [b]	1.2	0.4	88.8	8120	1.56
Meta-Bz	**CHO**	Bulk [b]	2.4	0.4	86.9	8490	1.60
Meta-Bz	**CHO**	Bulk [b]	3.8	0.4	84.6	8030	1.63
Meta-Bz	**CHO**	Bulk [b]	5.1	0.4	86.0	8750	1.66
Para-Bz	**CHO**	Bulk [c]	12	sunlight	86.2	2770	1.97
Meta-Bz	**CHO**	Bulk [c]	12	sunlight	91.6	4230	1.66

[a] 4h irradiation at 405 nm in CH_2Cl_2. [b] 20 min irradiation at 405 nm. [c] 20 min sunlight exposure (1.2 mW cm^{-2}, 365 nm detector, Shanghai 12:00 PM, May 20, 2013). [d] determined by gravimetry. [f] determined by GPC.

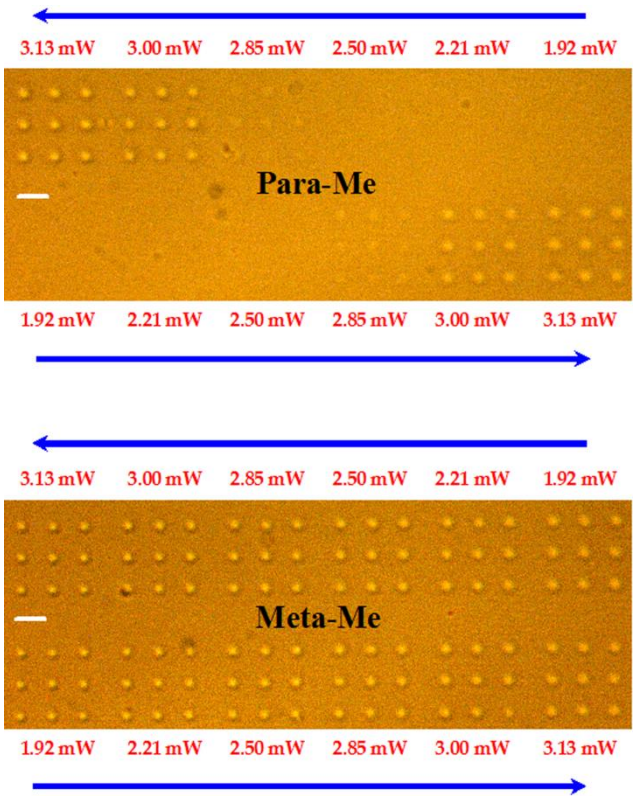

Fig. 4 Two-photon polymerization voxels obtained with point-by-point exposures at various exposure powers (λ_{exc}: 800 nm, exposure duration: 10 ms. Diepoxide resin containing 0.4 wt % of PAG.). Scale bars: 5 µm.

As depicted in Fig. S7, the same behaviours are observed with the photopolymerization of cyclohexene oxide (CHO). For this monomer, it should be noted that the final conversions of all formulations level off and reach values in the 80-90 % range. It can be ascribed to a much higher reactivity of CHO as compared to the difunctional EPOX mononer[51,60,61]. The differences in reactivity observed between the photoacid generators upon one-photon polymerization can be also demonstrated locally upon two-photon induced polymerization process at 800 nm. Fig. 4 and S8 show several sequences of 3 × 3 polymerized microdots generated upon two-photon excitation at 800 nm using the diepoxide formulations. In this point-by-point exposure method[62-67], the incident power is gradually decreased with a fixed exposure time of 10 ms to evaluate the minimum deposited energy below which the polymerization can not be observed. This latter parameter is the two-photon polymerization threshold (E_{th})[63, 66] and the corresponding values are listed in Table 2. Here also, the evolution of the two-photon polymerization threshold parallels with that of $\Phi_H^+.\delta_{800nm}$. Para-Me is obviously the less two-photon reactive PAG and therefore exhibits the highest E_{th}. On the other hand, meta PAG are the most reactive photoinitiators with a two-photon polymerization threshold which is 2.5-fold lower than that of Para-Me. Finally, Para-Bz presents an intermediate reactivity which agrees with the relative value observed for $\Phi_H^+.\delta_{800nm}$.

A series of polymers obtained from photopolymerization of cyclohexene oxide (CHO) or butyl vinyl ether (BVE) monomers have been characterized by GPC. Para-Bz and Meta-Bz were used respectively as moderate and highly reactive visible photoinitiators. Moreover, several experimental and processing factors have modified to correlate their respective influence on the final characteristic of the polymers (e.g. M_n and PDI). All experimental conditions and results are reported in Table 3. It should be first emphasized that the final properties of the polymers are both dependent on the nature of photoinitiators and the irradiation intensities. At low intensity (i.e. 0.2 mW.cm^{-2}), the photopolymerization with Meta-Bz leads to polymers with higher M_n and better polydispersities than those obtained using Para-Bz. Moreover, a strong increase of the irradiation intensity dramatically impacts the properties of the polymers obtained using Meta-Bz. For instance, the polyether produced from BVE / Meta-Bz undergoes an 8.4-fold decrease of M_n with a 1.3-fold increase of the PDI when the irradiation intensity is multiplied by a factor 10. Such a detrimental effect can be observed with CHO too and should be attributed to a reduction of the photoreactivity of Meta-Bz consecutive to a fast photobleaching process which does not produce any proton. As shown in Table 3, increasing the amount of Meta-Bz from 1.2 to 5.1 wt % in CHO has no significant effects on characteristics of final polymer in bulk polymerization. Finally, the remarkable photoreactivities of Meta-Bz and Para-Bz make them suitable candidates for cationic photopolymerization under sunlight exposure. This simple

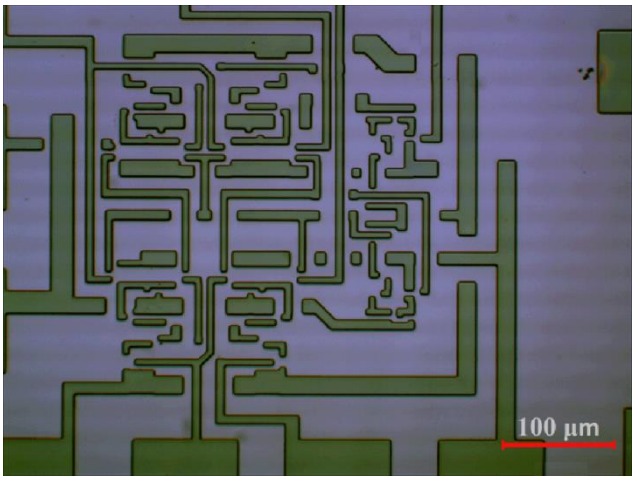

Fig. 5 Example of a microcircuit written upon one-photon lithography using SU-8 resin containing Meta-Bz (1 wt %). (λ_{exc}: 405 nm, irradiation dose: 200 µJ cm^{-2}).

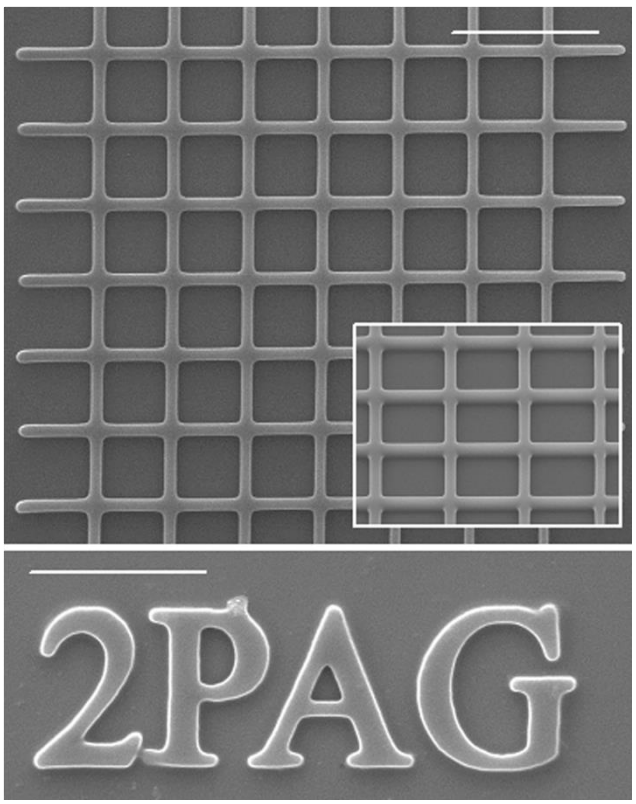

Fig. 6 SEM images of a µ-grid and a Logo fabricated upon excitation at 800 nm (< P > = 15 mW, v = 5 µm s^{-1}). Inset: Tilted view (θ = 45 °). Formulation: SU-8 resin with Meta-Bz (0.4 wt %). Scale bars: 20 µm.

irradiation mode which constitutes an important challenge in the context of energy conservation[9,10] has been performed using CHO. As shown in Table 3, the photopolymerization under sunlight exposition leads to high conversion of epoxide functions (> 80 %). Moreover, the properties of the polymers are clearly similar to those obtained under monochromatic conditions.

One and two-photon lithography

To finally demonstrate the potential applications of these π-conjugated photoacid generators for the one and two-photon microfabrication, several 2D microstructures were produced using SU-8 resin (Scheme 3). This highly viscous epoxy-based negative photoresist is for instance largely employed in microelectronics[4,5]. The resin was mixed with Meta-Bz (1 wt %) and spin-coated on Si substrates leading to micrometer-thick films. Fig. 5 shows the optical transmission microscopy image of a photo patterned microcircuit which was developed after visible irradiation of the photoresist (λ_{exc} = 405 nm). Such a light-imprinting method is based on the transfer of a geometric pattern on the film using a photomask. Interestingly, the same film preparation and development have been used for two-photon lithography. Fig. 6 shows the scanning electron microscope (SEM) images of two arbitrary 2D-microstructures which were written at 800 nm. The regular periodic array exhibits lines width of about 1.6 µm which is in good accordance with the optical spatial dimension of the focalized point (0.65 NA objective). Hence, from these two distinctive lithography strategies, we successfully demonstrate the potential interest of these new and highly reactivity photoacid generators for some relevant applications related to the microelectronics technology.

Conclusion

The photoreactivity of a new series of π-conjugated sulfonium-based photoacid generators have been evaluated. We showed that the para-to-meta positioning effect of the sulfonium substituent induces slight hypsochromic and hypochromic effects of the linear absorption bands without any detrimental impact on non-linear absorption properties but leads to a strong increase of the quantum yield for acid generation. A photolysis mechanism has been proposed and is based on a photoinduced electron-transfer S–C bond cleavage yielding a π-conjugated radical cation and a neutral carbon-centered radical. These intermediate species subsequently recombine together with the release of a protic acid. From a practical point of view, we also demonstrated that the photoinitiating performances of the PAG and the properties of the final photopolymers correlate very well with the relative reactivities of these photoinitiators. Finally, we show that this new series is of potential interest for microfabrication technologies and can be both employed for one and two-photon activation methods.

Acknowledgements

This work was supported by the National Natural Science Foundation of China (20902069, 51173134, 21074094) and Fundamental Research Funds for the Central University of Tongji University (0500219159). Supports from the Agence Nationale de la Recherche "Projet Blanc: *2PAGmicrofab* (ANR-BLAN-0815-03) " are also gratefully acknowledged.

Notes and references

[a] *School of Materials &Engineering, Tongji University, 4800 CaoAn Road, Shanghai, China. Fax: 86 21 69580143XXXX; Tel: 86 21 69580143; E-mail: mingjin@tongji.edu.cn*
[b] *Institut de Science des Matériaux de Mulhouse, UMR CNRS 7361, Université de Haute-Alsace, 15 rue Jean Starcky, 68057 Mulhouse, France. E-mail: jean-pierre.malval@uha.fr*
[c] *Institut de Chimie et des Matériaux Paris-Est, UMR 7182, 2-8 rue Henri Dunant, 94320 Thiais. Université Paris-Est Créeil Val de Marne, France.*

[d] *Laboratoire de Spectrométrie Physique, UMR CNRS 5588. Université Joseph Fourier, 38402 Saint Martin d'Hères, France.*
[e] *Laboratoire de Spectrochimie Infrarouge et Raman, UMR CNRS 8516. Université des Sciences et Technologies de Lille. 59655 Villeneuve d'Ascq Cedex*

† Electronic Supplementary Information (ESI) available: Fluorescence spectra, UV-Vis spectra of precursors, ^{1}H NMR, HPLC, MS, Photolysis, and one- and two-photon polymerizations data.
See DOI: 10.1039/b000000x/

1. J. V. Crivello, *J. Polym. Sci. Part A: Polym. Chem.*, 1999, **37**, 4241-4254.
2. J. V. Crivello and M. Sangermano, *J. Polym. Sci. Part A: Polym. Chem.*, 2001, **39**, 343-356.
3. J. P. Fouassier, D. Burr and J. V. Crivello, *J. Macromol. Sci. Part A*, 1994, **31**, 677-701.
4. E. Reichmanis, F. M. Houlihan, O. Nalamasu and T. X. Neenan, in *Polymers for Microelectronics*, American Chemical Society, 1993, pp. 2-24.
5. E. Reichmanis and F. Thompson Larry, in *Polymers in Microlithography*, American Chemical Society, 1989, pp. 1-24.
6. J.-P. Malval, F. Morlet-Savary, X. Allonas, J.-P. Fouassier, S. Suzuki, S. Takahara and T. Yamaoka, *Chem. Phys. Lett.*, 2007, **443**, 323-327.
7. J.-P. Malval, S. Suzuki, F. Morlet-Savary, X. Allonas, J.-P. Fouassier, S. Takahara and T. Yamaoka, *J. Phys. Chem. A*, 2008, **112**, 3879-3885.
8. M. Shirai and M. Tsunooka, *Prog. Polym. Sci.*, 1996, **21**, 1-45.
9. J. V. Crivello, *J. Macromol. Sci. Part A*, 2009, **46**, 474-483.
10. J. V. Crivello and U. Bulut, *J. Polym. Sci. Part A: Polym. Chem.*, 2005, **43**, 5217-5231.
11. J. Lalevée, M.-A. Tehfe, A. Zein-Fakih, B. Ball, S. Telitel, F. Morlet-Savary, B. Graff and J. P. Fouassier, *ACS Macro Lett.*, 2012, **1**, 802-806.
12. B. H. Cumpston, S. P. Ananthavel, S. Barlow, D. L. Dyer, J. E. Ehrlich, L. L. Erskine, A. A. Heika, S. M. Kuebler, I.-Y. S. Lee, D. McCord-Maughon, J. Qin, H. Röckel, M. Rumi, X.-L. Wu, S. R. Marder and J. W. Perry, *Nature*, 1999, **398**, 51-54.
13. S. Kawata, H.-B. Sun, T. Tanaka and K. Takada, *Nature*, 2001, **412**, 697-698.
14. C. N. LaFratta, J. T. Fourkas, T. Baldacchini and R. A. Farrer, *Angew. Chem. Int. ed*, 2007, **46**, 6238-6258.
15. H.-B. Sun and S. Kawata, *Two-Photon Photopolymerization and 3D Lithographic Microfabrication*, Berlin, 2004.
16. J.-D. Cho and J.-W. Hong, *Eur. Polym. J.*, 2005, **41**, 367-374.
17. J. Narewska, R. Strzelczyk and R. Podsiadly, *J. Photochem. Photobiol. A*, 2010, **212**, 68-74.
18. G. Manivannan and J. P. Fouassier, *J. Polym. Sci. Part A: Polym. Chem.*, 1991, **29**, 1113.
19. C. Li, L. Luo, S. Wang, W. Huang, Q. Gong, Y. Yang and S. Feng, *Chem. Phys. Lett.*, 2001, **340**, 444-448.
20. P. S. Billone, J. M. Park, J. M. Blackwell, R. Bristol and J. C. Scaiano, *Chem. Mater.*, 2009, **22**, 15-17.
21. J. V. Crivello, *J. Polym. Sci. Part A: Polym. Chem.*, 2007, **45**, 3759-3769.
22. J. V. Crivello and S. Liu, *Chem. Mater.*, 1998, **10**, 3724-3731.
23. J. V. Crivello, S. Rajaraman, W. A. Mowers and S. Liu, *Macromol. Symp.*, 2000, **157**, 109-120.
24. Y. Y. Durmaz, N. Moszner and Y. Yagci, *Macromolecules*, 2008, **41**, 6714-6718.
25. J. Lalevée, N. Blanchard, M. El-Roz, B. Graff, X. Allonas and J. P. Fouassier, *Macromolecules*, 2008, **41**, 4180-4186.
26. J. Lalevée, A. Dirani, M. El-Roz, X. Allonas and J. P. Fouassier, *J. Polym. Sci. Part A: Polym. Chem.*, 2008, **46**, 3042-3047.
27. J. Lalevée, M. El-Roz, X. Allonas and J. Pierre Fouassier, *J. Polym. Sci. Part A: Polym. Chem.*, 2008, **46**, 2008-2014.
28. D. Tunc and Y. Yagci, *Polym. Chem.*, 2011, **2**, 2557-2563.
29. Y. Yagci and S. Denizligil, *J. Polym. Sci. Part A: Polym. Chem.*, 1995, **33**, 1461-1464.
30. G. Yilmaz, S. Beyazit and Y. Yagci, *J. Polym. Sci. Part A: Polym. Chem.*, 2011, **49**, 1591-1596.
31. Y. Chen, T. Yamamura and K. Igarashi, *J. Polym. Sci. Part A: Polym. Chem.*, 2000, **38**, 90-100.
32. D. Dossow, Z. Qin Qin, G. Hizal, Y. Yagci and W. Schnabel, *Polymer*, 1996, **37**, 2821-2826.
33. E. W. Nelson, T. P. Carter and A. B. Scranton, *Macromolecules*, 1994, **27**, 1013-1019.
34. E. W. Nelson, T. P. Carter and A. B. Scranton, *J. Polym. Sci. Part A: Polym. Chem.*, 1995, **33**, 247-256.
35. M. R. Rodrigues and M. G. Neumann, *Macromol. Chem. Phys.*, 2001, **202**, 2776-2782.
36. Y. Yagci and Y. Hepuzer, *Macromolecules*, 1999, **32**, 6367-6370.
37. K. D. Belfield, K. J. Schafer, Y. Liu, J. Liu, X. Ren and E. W. V. Stryland, *J. Phys. Org. Chem.*, 2000, **13**, 837-849.
38. K. D. Belfield and K. J. Schafer, *Chem. Mater.*, 2002, **14**, 3656-3662.
39. S. M. Kuebler, K. L. Braun, W. Zhou, J. K. Cammack, T. Yu, C. K. Ober, S. R. Marder and J. W. Perry, *J. Photochem. Photobiol. A*, 2003, **158**, 163-170.
40. L. Steidl, S. J. Jhaveri, R. Ayothi, J. Sha, J. D. McMullen, S. Y. C. Ng, W. R. Zipfel, R. Zentel and C. K. Ober, *J. Mater. Chem.*, 2009, **19**, 505-513.
41. R. Xia, J.-P. Malval, M. Jin, A. Spangenberg, D. Wan, H. Pu, T. Vergote, F. Morlet-Savary, H. Chaumeil, P. Baldeck, O. Poizat and O. Soppera, *Chem. Mater.*, 2012, **24**, 237-244.
42. C. O. Yanez, C. D. Andrade and K. D. Belfield, *Chem. Comm.*, 2009, 827-829.
43. T. Yu, C. K. Ober, S. M. Kuebler, W. Zhou, S. R. Marder and J. W. Perry, *Adv. Mater.*, 2003, **15**, 517-521.
44. W. Zhou, S. M. Kuebler, K. L. Braun, T. Yu, J. K. Cammack, C. K. Ober, J. W. Perry and S. R. Marder, *Science*, 2002, **296**, 1106-1109.
45. C. O. Yanez, C. D. Andrade, S. Yao, G. Luchita, M. V. Bondar and K. D. Belfield, *ACS Appl. Mater. Interfaces*, 2009, **1**, 2219-2229.
46. F. D. Saeva, D. T. Breslin and H. R. Luss, *J. Am. Chem. Soc.*, 1991, **113**, 5333-5337.
47. F. D. Saeva, D. T. Breslin and P. A. Martic, *J. Am. Chem. Soc.*, 1989, **111**, 1328-1330.
48. F. D. Saeva, E. Garcia and P. A. Martic, *J. Photochem. Photobiol. A*, 1995, **86**, 149-154.
49. F. D. Saeva and B. P. Morgan, *J. Am. Chem. Soc.*, 1984, **106**, 4121-4125.
50. M. Jin, H. Xu, H. Hong, J.-P. Malval, Y. Zhang, A. Ren, D. Wan and H. Pu, *Chem. Comm.*, 2013, **49**, 8480-8482.
51. W. Zhou, S. M. Kuebler, D. Carrig, J. W. Perry and S. R. Marder, *J. Am. Chem. Soc.*, 2002, **124**, 1897-1901.
52. R. Meech and D. Phillips, *J. Photochem.*, 1983, **23**, 193–217.
53. J. V. Crivello and R. Narayan, *Macromolecules*, 1996, **29**, 439-445.
54. R. P. Subrayan, J. W. Kampf and P. G. Rasmussen, *J. Org. Chem.*, 1994, **59**, 4341-4345.
55. G. Pohlers, J. C. Scaiano and R. Sinta, *Chem. Mater.*, 1997, **9**, 3222-3230.
56. P. Beak and T. A. Sullivan, *J. Am. Chem. Soc.*, 1982, **104**, 4450-4457.
57. F. D. Saeva, B. P. Morgan and H. R. Luss, *J. Org. Chem.*, 1985, **50**, 4360-4362.
58. X. Wang, F. D. Saeva and J. A. Kampmeier, *J. Am. Chem. Soc.*, 1999, **121**, 4364-4368.
59. D. Griller and D. D. M. Wayner, *Pure Appl. Chem.*, 1989, **61**, 717-724.
60. J. Kreutzer, K. D. Demir and Y. Yagci, *Eur. Polym. J.*, 2011, **47**, 792-799.
61. Y. Yagci, S. Jockusch and N. J. Turro, *Macromolecules*, 2010, **43**, 6245-6260.
62. M. Jin, J. P. Malval, D. L. Versace, F. Morlet-Savary, H. Chaumeil, A. Defoin, X. Allonas and J. P. Fouassier, *Chem. Comm.*, 2008, **48**, 6540-6542.
63. K.-S. Lee, D.-Y. Yang, S. H. Park and R. H. Kim, *Polym. Adv. Technol.*, 2006, **17**, 72-82.
64. G. Lemercier, J. C. Mulatier, C. Martineau, R. Anémian, C. Andraud, I. Wang, O. Stephan, N. Amari and P. L. Baldeck, *C.R. Chimie*, 2005, **8**, 1308-1316.

65. J.-P. Malval, F. Morlet-Savary, H. Chaumeil, L. Balan, D.-L. Versace, M. Jin and A. Defoin, *J. Phys. Chem. C*, 2009, **113**, 20812-20821.
66. C. Martineau, G. Lemercier, C. Andraud, I. Wang, M. Bouriau and P. L. Baldeck, *Synth. Met.*, 2003, **138**, 353-356.
67. S. A. Pruzinsky and V. Braun, *Adv. Funct. Mater.*, 2005, **15**, 1995-2004.

Table of contents

D-π-A type π-conjugated photoacid generators through para-to-meta substitution strategy show high efficiency in photoinitiated cationic polymerizations by 405 nm and 800 nm excitation.